Research Square

Preprints are preliminary reports that have not undergone peer review.
They should not be considered conclusive, used to inform clinical practice,
or referenced by the media as validated information.

In Vitro Culture and Draft Genome Assembly of Monographella maydis Predict a Molecular Driver of Its Sexual Fitness in Maize Tar Spot Disease

Akshaya K. Biswal
University of Georgia
Susana D. Arteaga-Quiroz
Higher Education School of Apan, Autonomous University of Hidalgo
Sameer Pokhrel
University of Georgia
Irma Martínez
National Autonomous University of Mexico
Libia F. Gómez-Trejo
University of Nebraska–Lincoln
Carlos Muñoz Zavala
International Maize and Wheat Improvement Center (CIMMYT)
Peggy Ozias-Akins
University of Georgia
Amos E. Alakonya
a.alakonya@cgiar.org

International Maize and Wheat Improvement Center (CIMMYT-SENEGAL)

Research Article

Keywords:

Posted Date: May 15th, 2026

DOI: https://doi.org/10.21203/rs.3.rs-9543400/v1

License: This work is licensed under a Creative Commons Attribution 4.0 International License.
Read Full License

Additional Declarations: No competing interests reported.

In Vitro Culture and Draft Genome Assembly of *Monographella maydis* Predict a Molecular Driver of Its Sexual Fitness in Maize Tar Spot Disease

Akshaya K. Biswal[1,2], Susana D. Arteaga-Quiroz[3], Sameer Pokhrel[2], Irma Martínez[4], Libia F. Gómez-Trejo[5], Carlos Muñoz Zavala[6], Peggy Ozias-Akins[1,2], Amos E. Alakonya[7]

[1]: Department of Horticulture, University of Georgia, 2353 Rainwater Road, Tifton, GA 31793-5766, USA

[2]: Institute of Plant Breeding, Genetics and Genomics (IPBGG), University of Georgia, 2353 Rainwater Road, Tifton, GA 31793-5766, USA

[3]: Higher Education School of Apan, Autonomous University of Hidalgo, Campo de Tiro, 43920 Apan, Hidalgo, Mexico

[4]: Center for Genomic Sciences, National Autonomous University of Mexico, 62210 Cuernavaca, Morelos, Mexico

[5]: Center for Plant Science Innovation and Department of Plant Pathology, University of Nebraska-Lincoln, Lincoln, NE, 68588, USA

[6]: International Maize and Wheat Improvement Center (CIMMYT), Km 45, Carretera Mexico-Veracruz, El Batan, Texcoco, 56237, Mexico

[7]: Dryland Crops Program, International Maize and Wheat Improvement Center (CIMMYT-SENEGAL) ISRA/CERAAS, Km 7.5 Route de Khombole, P.B. 3320, Thiés, Senegal

Email: a.alakonya@cgiar.org

Abstract

Tar Spot Complex (TSC) is a devastating foliar disease of maize that threatens global food security, causing yield losses of up to 50%. While the disease is initiated by *Phyllachora maydis*, the "fisheye" necrosis that intensifies disease severity is attributed to *Monographella maydis*. Historically, the precise role of *M. maydis* has remained elusive due to a lack of reliable *in vitro* culture systems and genomic resources. This study reports the first successful isolation and reproducible *in vitro* culture of *M. maydis*, identifying V8 agar as an optimal medium for mycelial growth and sporulation.

Using PacBio long-read sequencing technology, we generated a high-quality 39.8 Mb genome assembly for *M. maydis*, predicting 10,228 protein coding genes, 227 non-coding RNAs, 175 tRNAs and 45 rRNAs. Functional annotation identified a diverse repertoire of secreted proteins and multiple biosynthetic gene clusters, likely involved in the tar spot disease pathosystem interaction. Phylogenomic analysis confirmed that *M. maydis* is distinct from *P. maydis*, supporting a synergistic rather than evolutionary relationship between the two fungi. Furthermore, the identification of a conserved *adenosine deaminase* residue (H352) suggests potential for A-to-I RNA editing during sexual reproduction. Finally, we report the use of ITS1 and ITS4 primer pair for successful detection of *M. maydis* from infected leaf tissues. These findings provide a foundational genomic and microbiological framework for improving molecular diagnostics and developing effective management strategies to mitigate the economic impact of TSC on maize production.

Background

Tar spot complex (TSC) is a destructive foliar disease of maize causing up to 50% yield loss, affecting both the maize growers and regional food security in the Americas [1]. While the tar spot disease can appear at any developmental stage of the plant, appearance of tar spot before or during the flowering stage leads to inadequate formation of the inflorescence, which can result in complete crop loss [2]. The TSC disease causes significant yield loss and a challenge for farmers in different countries of the American continent such as Mexico, Guatemala, El Salvador, Colombia, Nicaragua, Honduras, Bolivia, Costa Rica, Dominican Republic, Panama, Peru, Puerto Rico, Venezuela [3, 4]. Leaving the infected crop residue (like leaves and stalks) on the farm or near the storage area allows overwintering of the pathogen and release of spores during the following growing season [5]. Harvesting machinery, if not properly sanitized, can also help in spore dispersal to uninfected fields.

Maize tar spot is also continuously spreading to newer horizons. In 2015, it was first reported in the USA [6]. In 2024, the yield loss due to tar spot disease in the USA reached nearly 1.3 billion dollars; almost doubling the losses between 2018 and 2024 [7]. Since many developing countries rely on the import of maize originating from the USA, there is a potential of disseminating the disease to other countries through infected debris in grains [8].

TSC was first reported in Mexico over a century ago and two fungi, *Phyllachora maydis* and *Coniothyrium phyllachorae* were identified to be involved in its formation [9]. *Monographella maydis* was later found inside the necrotic areas of the infected leaf [10]. While *P. maydis* is believed to initiate the tar spot, subsequent co-infection by *M. maydis* is known to cause the damaging fisheye like necrosis around the tar spot or simply the fisheye symptom (Fig. 1) [4]. Accordingly, inoculation of *M. maydis* conidia enhances the severity of the tar spot disease under field conditions reinforcing the temporal sequence of infection of this synergistic plant pathogen interaction.

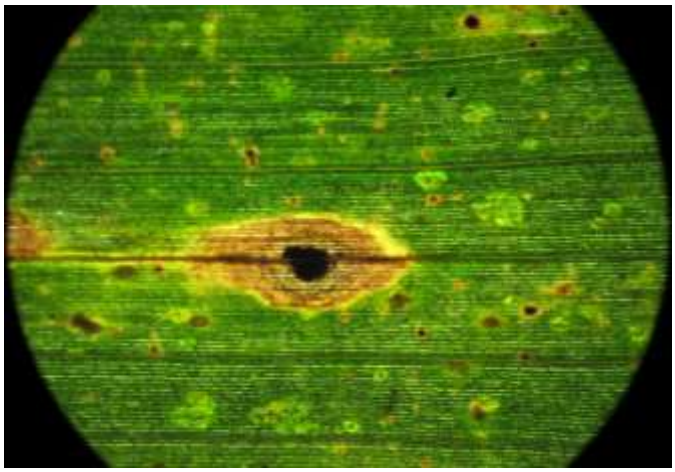


Figure 1: Fisheye symptom, seen through a stereo microscope.

The fisheye symptoms appear 2–7 days after *P. maydis* colonization, followed by the proliferation of *M. maydis*, which eventually predominates in the lesions and coincides with empty perithecia of *P. maydis* [4]. Thus, *M. maydis* that drives lesion expansion, intensifies infection, and underpins the destructive nature of the tar spot complex although *P. maydis* initiates the disease. The conidia of *M. maydis* survive as long as 109 days under ambient conditions [11]. This means *M. maydis* can overwinter on debris and infect the maize leaves as soon as the *P. maydis* starts to colonize.

However, a few recent reports have challenged the role of *M. maydis* in development of fisheye symptoms in tar spot disease of maize in the United States and Mexico [12, 13]. In the absence of a reproducible *in vitro* culture system and reliable molecular markers to clearly distinguish between these fungal species, these studies have contributed to greater ambiguity rather than resolving the identity of the causal agents of TSC disease, particularly with respect to the more destructive fisheye symptom.

Significant progress has been made in studying the molecular nature of *P. maydis* infection because of the availability of molecular markers and recent availability of its genome sequence [14–16]. However, the biology, pathogenic nature and molecular characteristics of *M. maydis* have not yet been delineated so far, limiting our capacity to develop accurate diagnostic tools and effective management strategies to limit yield loss. The lack of a reliable *in vitro* culture protocol and genome sequence of *M. maydis* have remained the primary limitations to these studies.

The *M. maydis* was first morphologically characterized by Müller & Samuels [10] as a pyrenomycetous fungus, found within the necrotic areas of tar spot. Its ascomata are initially light colored but become brownish with age. The asci inside the ascomata are unitunicate and carry an amyloid apical ring. Each ascus contains eight colorless, phragmosporous ascospores. Ascomata are accompanied by light-colored sporodochia from which annellidic conidiogenous cells arise and produce narrowly clavate to cylindrical, hyaline, phragmosporous conidia. This species was placed in *Monographella* by Petrak [17]. The associated anamorph was a species of *Microdochium* H. Sydow, similar to the *Microdochium* anamorph of *Monographella nivalis* [10].

Monographella spp. belongs to the phylum Ascomycota and possess septate hyphae exhibiting both sexual (telomorph) and asexual (anamorph) forms of reproduction in their life cycle [18]. The teleomorph of *M. maydis* produces flask-shaped perithecia with an ostiole that allows release of the asci. Each ascus carries 8 trisepted ascospores. The anamorph *Microdochium maydis* forms tri-sepsted conidia, crucial for asexual reproduction. Though these are hyaline at the beginning, they turn darker on maturity.

Thus, this study was designed to isolate and characterize *M. maydis* through whole-genome sequencing and functional annotation. This outcome represents the first comprehensive report of *in vitro* culture and characterization of *M. maydis,* providing critical insights into genomics and fungal pathology, setting up a platform for further studies to confirm its role in TSC and its interactions with other co-colonizing fungi. Additionally, we report the first molecular marker for early detection of *M. maydis* in TSC. Combinedly, these results open a new avenue for molecular diagnostics, host–pathogen interaction studies, and disease management strategies in maize.

Results and discussion

Isolation of *Monographella maydis* and optimization of *in vitro* culture conditions

After incubating the infected leaf samples for approximately one week in a humid chamber, perithecia and sporodochia, growing on the fish-eye lesions, were isolated with fine sterile needles

and cultured on media plates. Although *Microdochium maydis* (the anamorph of *M. maydis*) could be morphologically mistaken for *Fusarium* spp., distinctive characteristics such as the round triseptate sporodochia of *Microdochium* versus the pointed sporodochia of *Fusarium*, which were divided by a greater number of septa, allowed for accurate differentiation (Fig. 2a, b, c).

Among four different media that were tested, the uniform mycelial development and sporulation were obtained on V8 medium, which was selected for all further culturing and subculturing (Fig. 2d). In other three media, the fungal growth remained limited and patchy and was also non-reproducible. Three isolates (plates MNG128, MNG133, and MNG137), all derived from leaf sample #86, showed consistent growth and produced perithecia *in vitro*. Perithecia from these plates were preserved on sterile filter paper at 4°C for further use.

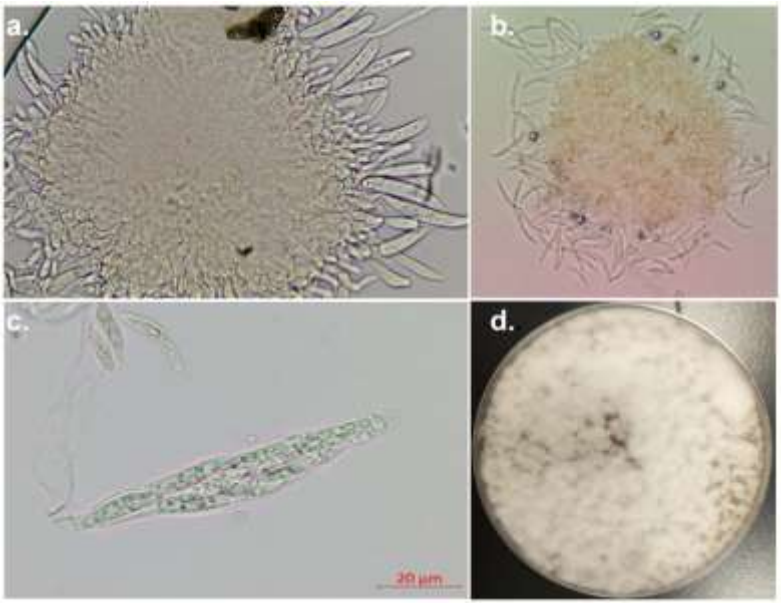


Figure 2: a) *Microdochium maydis* sporodochia; b) *Fusarium sp.* sporodochia found in the same leaf; c) Isolated ascus as seen through a compound microscope; eight ascospores, visible inside the ascus are characteristic of *Monographella*. Another ascus (almost empty) can be seen; these are unitunicated and d) Mycelia from the subculture of the original strains of *M. maydis* (isolate MNG133).

Identification of *Monographella maydis*

PCR primers targeting the highly conserved ribosomal DNA (rDNA), flanking the Internal Transcribed Spacer (ITS) region allow amplification across broad fungal taxa and have been used for clear identification of different fungal species [19, 20]. The PCR amplification using ITS1 and ITS4 primers produced clear bands between 500 – 600 bp (Fig. 3). The amplicon of *Monographella* was slightly smaller than that of *Aspergillus flavus* that was used as a negative control. Amplicons obtained from isolates MNG128, MNG133, and MNG137 exhibited the same fragment length.

The gel eluted fragments of all three ITS-specific PCR products were sequenced at Macrogen, Korea (Supplementary fig. 1). Analysis of these sequences using NCBI BLAST identified *Microdochium* as the best match with above 95% identity and nearly 97% coverage, confirming the identity of the fungal isolates.



Figure 3: Differentiation between *Monographella maydis* and *Aspergillus flavus* by PCR: The genomic DNA was amplified using ITS1 and ITS4 primer pair and separated in a 1% agarose gel by running for 45 min at 100 V. The *M. maydis* isolates (128, 133, 137 and +) show slightly smaller bands than *A. flavus*. The '+' indicates an isolate that was characterized morphologically during the initial isolation.

Extraction of high-quality DNA and PacBio long-read sequencing

While good quality DNA is the basic requirement for the long-read PacBio sequencing, many fungal species, especially filamentous fungi, produce robust DNases that are not fully inactivated or removed during standard extraction protocols. The extraction process is also challenged by the complex fungal cell wall composition, primarily consisting of chitin, glucans, and glycoproteins [21]. Therefore, the Quick-DNA™ Fungal/Bacterial Miniprep Kit (Zymo Research, USA) and an *in-house* CTAB method were tested for the initial genomic DNA extraction. The Quick-DNA™ kit produced low molecular weight DNA (~5 kb) (Supplementary fig. 2a) and the concentration was not sufficient for long-read sequencing while the alternative protocol, based on Phenol:Chloroform:Isoamyl alcohol (25:24:1) extraction, proved more efficient and cost-effective, producing higher molecular weight DNA (>15 kb) and concentration (>200 ng/µl), suitable for third-generation sequencing (Supplementary fig. 2b). High quality library preparation and genome sequencing at the depth of 250X was performed at Novogene and 21.5, 17.8 and 27.3 Gb of raw read data was received in bam format for isolates MNG128, MNG133 and MNG137 respectively.

Genome assembly and quality assessment

A consensus genome assembly (NCBI BioSample accession: SAMN56535211) was generated using Canu Version 2.2 [22]. Total 71 contigs were generated with a total length of 39,490,855 bp. The BUSCO (Benchmarking Universal Single-Copy Orthologs) Version 5.83 search found 99.9% completeness of the assembly [23, 24]. Our search included 758 universal single-copy ortholog genes (n) of which 748 (98.7%) were single-copy, 9 (1.2%) were duplicated while only one (0.1%) was missing and none were fragmented. The contig N50 value, defined as the length of the shortest contig, such that 50% of the total genome assembly is contained in contigs of that length or longer, was 3 Mb (Supplementary table 1).

The QUAST analysis of the assembly showed that more than 60% of the contigs were larger than 10 Kb in length while contigs of more than 50 Kb contributed more than 25% of all contigs (**Error! Reference source not found.**) [25]. The overall GC content was 54.21%. Ascomycetes exhibit a

wide range of genomic GC content, generally from around 38% to over 50%. While genomes of some species like *Saccharomyces cerevisiae* (budding yeast) contain about 38% GC, others show significantly higher percentages, illustrating substantial evolutionary diversity in base composition influenced by mutational biases and selection. The GC content of *M. maydis* was significantly lower than *P. maydis* (47.2%) and major *Fusarium* species associated with maize, such as *Fusarium verticillioides* and *Fusarium graminearum*, which have about 48% GC content [14, 26, 27].

The QUAST size-threshold statistics indicate that the assembly is highly contiguous and contains very few small contigs. The total assembly length remained the same after removing contigs less than 1,000 bp indicating that very short contigs are absent in the assembly. When the size thresholds were progressively increased (≥ 5 kb, ≥ 10 kb, ≥ 25 kb, and ≥ 50 kb), the total assembly length decreased only slightly at each step demonstrating that most of the genomic sequence was contained in large contigs (Supplementary table 2). Notably, even when only contigs ≥ 50 kb were considered, the retained length remained very close to the total assembly size, confirming that most of the genome was assembled into long, high-quality sequences. One single contig (~5.5 Mb) contributed 13.8% of the total assembly. Overall, these patterns reflected a robust and well-assembled genome with strong contiguity and minimal fragmentation.

The assembly consisted of 71 contigs totaling 39.6 Mb. The number of contigs and scaffolds remain the same since scaffolding was not performed. The absence of N bases, L50 and N50 values also reflect the high contiguity and relatively less fragmented nature of the assembly, generated from the long-read PacBio CLR data. This reference assembly represents the first genomic characterization of *Monographella maydis,* providing valuable information for understanding its pathogenic potential and evolutionary relationships within the TSC. The high-quality assembled genome will serve as the foundation for the subsequent functional annotation and phylogenomic analyses.

Presence of repeat and transposon elements

The RepeatMasker (version 4.2.3) analysis showed that 6.73% of the *M. maydis* genome consisted of repetitive sequences, including 5.47% interspersed repeats and 1.26 % simple sequence repeats (SSRs) [28]. Notably, the repeat content of *M. maydis* genome is over 8-fold lower than *P. maydis*. The repeat content in Ascomycetes fungi is highly variable, ranging from very low in yeasts to significant amounts in filamentous fungi, with transposable elements (TEs) acting as a major driver of this diversity. The significant differences in repeat content highlights distinct evolutionary strategies, genomic structures, and pathogenic lifestyles between these two maize pathogens.

The *M. maydis* genome also included approximately 2% DNA transposon elements (Supplementary table 3). The low percentage of DNA transposon elements suggest a relatively stable genome where Class II elements might be playing only a subtle role in genome evolution and regulation. It also contained 17 Long Interspersed Nuclear Elements (LINEs), but no Short Interspersed Nuclear Elements (SINEs).

Gene prediction and functional annotation

Building upon the obtained assembly, the next phase of the study focused on the structural and functional genome annotation of *M. maydis*, integrating multiple bioinformatic tools to predict gene models, assign functional roles, and explore the molecular basis of its interaction with the host and other fungi involved in the tar spot complex. The FunAnnotate pipeline and BLAST analysis predicted a total of 10,392 annotated genes, of which 10, 228 are protein coding. which is approximately 70% higher than *P. maydis* [14]. Rest 164 genes were identified as tRNA genes by the FunAnnotate pipeline. For accurate detection and functional prediction, we reanalyzed the genome with tRNAscan SE 2.0 [29, 30]. Total 175 Infernal-confirmed tRNAs were predicted by tRNAscan of which 166 were encoded standard 20 amino acids while 9 others were pseudogenes. *M. maydis* tRNA count was almost double of *P. maydis*. Additionally, 119 *M. maydis* tRNAs contained introns too. Total 227 non-coding RNA (ncRNA) loci were identified using Infernal (v1.1.5) with the Rfam database. Similarly, Barrnap (v0.9) identified 45 rRNA genes in the genome [31]. This indicates that gene prediction pipeline worked well and *M. maydis* has higher metabolic versatility than *P. maydis*.

To understand the biological blueprint of *M. maydis*, we identified 12,177 Pfam conserved domains in 7,543 genes (Table 1). The average Pfam count (1.2 per gene) is comparable to the average of 1.7 domains per gene in eukaryotes [32]. The high Pfam count suggests a complex life cycle with diverse metabolic capabilities (e.g., secondary metabolism, cell wall degradation, saprotrophic absorption of nutrients). Multidomain proteins are also common in fungi and play important roles in catalysis, signaling and interactions with the host [33].

We also identified 773 UniProt hits from our predicted proteins representing genes with known experimental functions (Table 1). However, there was a large difference between the number of Pfam domains and Uniprot hits. This indicates that most of the genes were recognizable by their Pfam domains, but the whole protein sequences might not have been documented before. This is common in fungal genomics because fungal diversity is vast and remains substantially under-sampled.

Table 1. Results of the structural and functional annotation of *M. maydis*

Category	Count
Annotated genes	10,392
Protein coding genes	10, 228
Total tRNA related genes	175
tRNAs coding standard amino acids	166
tRNA pseudogenes	9
tRNAs containing intron	119
ncRNA	227
rRNAs	45
Pfam domains	12,177
Pfam domain containing genes	7,543

UniProt hits	773
MEROPS entries	449
CAZy families	849
Predicted secreted proteins (SignalP)	970

Similarity searches against MEROPS database identified putative peptidase or protease-related proteins in the predicted *M. maydis* proteome. Of 511 total genes that showed a top MEROPS hit, 449 passed stringent filtering criteria (percent identity ≥ 30%, bit score ≥ 100 and e-values ≤ 1.0e-20) (Supplementary table 4). Nearly one third of these entries were secreted (Supplementary table 4). The top represented MEROPS proteins were *peptidases* that are crucial for fungal pathogenicity, nutrient acquisition and cellular signaling [34].

The Funannotation pipeline also identified 849 putative carbohydrate-active enzymes (CAZy) in *M. maydis* proteome, including 246 *glycoside hydrolases*, 81 *glycosyltransferases*, 99 with auxiliary activities, 31 *carbohydrate esterases*, 8 *polysaccharide lyases*, and 88 carbohydrate-binding modules. These enzymes may serve as virulence factors, allowing pathogens to degrade plant cell walls and penetrate host tissues using specialized infection structures [35–37]. Our analysis predicted 970 secreted proteins**,** which are short peptides, generally secreted out of the cells. These represent nearly ~9.5% of the total proteome.

Further analysis identified 252 of these CAZy proteins, belonging to the family of secreted proteins. The glycoside hydrolases (GH) family 76 (GH76) represented the highest portion of the secreted proteins. GH76 proteins are essential for fungal cell wall biosynthesis and pathogenic development, acting as endo-α-1,6-mannanases that remodel cell wall mannoproteins. In pathogens like *Pyricularia oryzae*, they are critical for appressorium maturation and host penetration [38]. Therefore, the overrepresentation of GH76 in the secreted CAZy proteins of *M. maydis* may be responsible for its fitness to thrive on maize leaves. GH18 and Auxiliary Activity Family 9 (AA9) represented the second and third highest represented class of secreted CAZy proteins (Supplementary Table 4).

Orthology analysis

KEGG Orthology (KO) analysis of *Monographella* proteins linked their roles to some key functions (Table 2). For example, we identified 30 *Glucokinase* orthologs in *Monographella* genome. *Glucokinase* facilitates the sugars assimilation that helps the fungus outcompete host cells for nutrients supporting the energetic demands during the infection [39, 40]. Inhibition of fungal *glucokinase* has been shown to inhibit growth of fungus *Diaporthe citri*, a pathogenic fungus affecting citrus [41].

Our genomic analysis identified 15 predicted *Glutamine synthetase* (GS) genes in *M. maydis.* GS is a critical regulator of fungal growth, conidiation, and oxidative stress resistance, as evidenced in pathogens like *Aspergillus flavus* [42]. Plant GS genes can also bolster resistance against pathogens like *M. oryzae.* Therefore, the outcome of an infection often depends on a metabolic

"tug-of-war" for glutamine. The presence of 15 GS genes suggests a robust metabolic strategy for the adaptation and virulence of *M. maydis*.

Adenosine deaminase (ADA) orthologs were the second highest populated enzymes in KO analysis. Our comparative ortholog analysis revealed a striking divergence in the ADA catalytic domains between *M. maydis* and *P. maydis*. The *M. maydis* ADA sequence retains a highly conserved catalytic motif, specifically the H352 residue similar to *FgTad2* ortholog in *F. graminearum* while this domain has been completely disturbed in *P. maydis* due to a large deletion [43] (Fig. 4). Genomic sequences for the *M. maydis* and the *P. maydis* genes could not be aligned due to low sequence similarities highlighting their possible complementarity in causing tar spot complex. Other known protein families with critical role in metabolic networks have been listed in Table 2 with their corresponding functions.

Table 2: Top 10 most frequent KOs.

KO ID	Count	Description
K00505	30	Glucokinase [EC:2.7.1.2]
K01426	24	Adenosine deaminase [EC:3.5.4.4]
K16261	21	FAD-dependent oxidoreductase
K01183	17	Alpha-glucosidase[EC:3.2.1.20]
K05349	15	Fungal zinc-finger transcription factor
K00799	15	Glutamine synthetase [EC:6.3.1.2]
K08286	14	F-box protein
K08141	14	Kinase protein
K00480	11	Cytochrome c oxidase subunit 1 [EC:7.1.1.9]
K01230	10	Beta-galactosidase [EC:3.2.1.23]

Functional implications of ADA polymorphism on sexual stage-specific A-to-I mRNA editing

Emerging evidences highlight importance of ADA in fungal sexual reproduction, metabolic survival, and potential immune evasion [44–46]. In *Fusarium* species, *FgTad2*, an adenosine-deaminase-acting-on-tRNA (ADAT), catalyzes Adenosine-to-Inosine (A-to-I) mRNA editing during sexual reproduction [47, 48]. A-to-I editing generates adenosine (A)-to-guanosine (G) substitutions in coding RNA, because the ribosome interprets I as G during translation. *FgTad2* proteins purified from perithecia show mRNA editing activities, but not from vegetative hyphae. In filamentous ascomycetes, the H352 residue is conserved and is indispensable for A-to-I mRNA editing that governs perithecial maturation and ascosporogenesis [43]. Accordingly, H352 of *FgTad2* is conserved in its orthologs of other filamentous ascomycetes such as *F. graminearum*, *N. crassa*, and *S. macrospora*, but not in Tad2 of *S. cerevisiae* that lack A-to-I editing (Fig. 4).

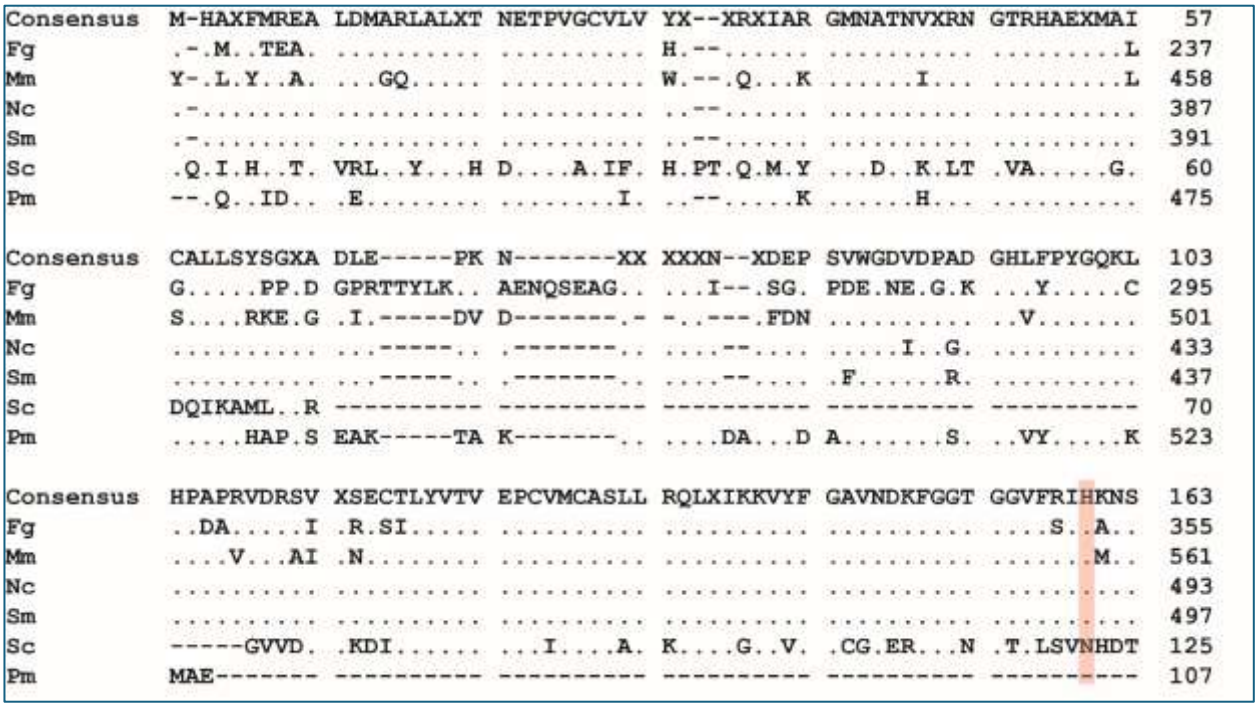


Figure 4: Alignment of the partial amino acid sequence of FgTad2 from *Fusarium graminearum* (*Fg*) and the predicted protein sequences from our genome assembly for *M. maydis* (Mm.7485_t) and *Phyllachora maydis (Pm)*. Orthologs from Sordariomycetes *Neurospora crassa* (Nc) and *Sordaria macrospora* (Sm) were included in comparison in which stage-specific A-to-I RNA editing also occurs during sexual reproduction. *Saccharomyces cerevisiae* (Sc) was added for comparison in which stage specific A-to-I RNA editing is not observed. The conserved H352 residue has been highlighted by the light pink rectangle. Dot (.) indicate consensus residue.

Sequence alignment of *M. maydis* and *P. maydis* orthologs revealed presence of the conserved H352 residue in *M. maydis* indicating its ability to catalyze mRNA editing. Interestingly, a large deletion was observed in the corresponding domain of *P. maydis* ortholog, effectively disrupting

the catalytic pocket. This structural impairment aligns with the significantly lower ascospore germination rates previously reported in *P. maydis* [5].

Other functions of ADA in *M. maydis* may include an advantage in metabolic evasion within the maize apoplast. By deaminating host-produced purine analogs or nucleoside-based defensive metabolites, *M. maydis* could effectively detoxify its local environment. In addition to facilitating its own survival, this enzymatic activity may also influence the broader dynamics of the maize tar spot complex by altering the chemical ecosystem in which *P. maydis* and other secondary pathogens persist [48]. While self-germination inhibition was suggested due to high spore densities, the lack of a functional deaminase motif in *P. maydis* may also be limiting its ability to neutralize host-produced purine analogs [5]. However, experimental verification is required to confirm the role of ADA in metabolic evasion.

The presence of a functional ADA in *M. maydis* is likely to support superior fitness through both sexual vigor and metabolic evasion while the impaired ADA in *P. maydis* may force a reliance on alternative survival strategies. This structural loss likely represents a specialized evolutionary trade-off and complementation between *P. maydis* and *M. maydis,* where the earlier could initiate the disease during the biotrophic phase while the latter has enhanced survival on the host during hemibiotrophic and necrotrophic phases.

Secondary metabolite analysis

Small bioactive compounds are produced by fungi as a part of their specialized mechanism to survive upon their hosts, crop debris and soil. Biosynthetic gene clusters are physically clustered groups of two or more genes that encode biosynthetic pathways for the production of a specialized metabolites [49]. Our antiSMASH analysis identified multiple biosynthetic gene clusters such as terpenes, polyketide synthases (such as T1PKS and T3PKS), and nonribosomal peptide synthetases (NRPS) that allow the production of many secondary metabolites, which are key mediators in plant-fungal interactions [50, 51].

Secondary metabolites play important roles in virulence and infection of plants, acting as toxins, compounds that affect the plant growth or its immune system, and for competing or having symbiotic relationships with other organisms [52–54]. Since antiSMASH prediction does not imply active production of these compounds, further quantitative experimental validation is required to establish the involvement and mode of action of these compounds in tar spot complex of maize.

Phylogenomic analysis

To infer evolutionary relationships between *P. maydis* and *M. maydis,* a phylogenetic tree was constructed using the whole proteome data. Two common maize fungi, *F. graminearum* and *F. verticilliodes* and three *Microdochium* species were also included in the tree. The phylogenetic tree branching showed that *P. maydis* is the most divergent taxon within the dataset (Fig. 5a). The remaining species formed a well-supported clade in which *M. maydis* clustered closely with *M.*

trichocladiopsis, suggesting a relatively recent common ancestor. Slightly deeper branches separate *M. bolleyi* and *M. nivale*, which group together as sister taxa.

The relatively low proteomic similarity between *Monographella* and *Phyllachora* species indicates that these are functionally divergent and their association is likely the result of a complex synergistic interaction rather than a shared evolutionary origin. Although both fungi co-occur within the same lesions, they appear to exploit the maize host using distinct biological strategies and molecular tools. This interaction likely reflects the progression of pathogenic phases in the tar spot complex. Accordingly, *P. maydis* initially establishes infection through a biotrophic phase, maintaining host tissue viability, which is followed by colonization by *M. maydis* exhibiting hemibiotrophic to necrotrophic behavior. The transition to necrotrophy ultimately drives tissue necrosis and lesion expansion, resulting in the characteristic fisheye symptoms associated with severe tar spot disease.

To further understand the genetic relationship among these species, a heatmap was constructed using the pairwise mash distance between individual species. The mash distance was calculated based on the genome-wide sequence similarity using Kmer-based comparison and genomes were clustered based on their genetic distances (Fig. 5b). The deep red colored blocks in the heat map clearly demonstrate that *M. maydis* is genetically very distant from *P. maydis*, and both *Fusarium* species. In contrast, its genome showed high similarity to all three *Microdochium* species, as expected. Combinedly, these analyses reveal significant genetic and functional differences between *M. maydis* and *P. maydis* and indicate mutualism rather than competition between them.

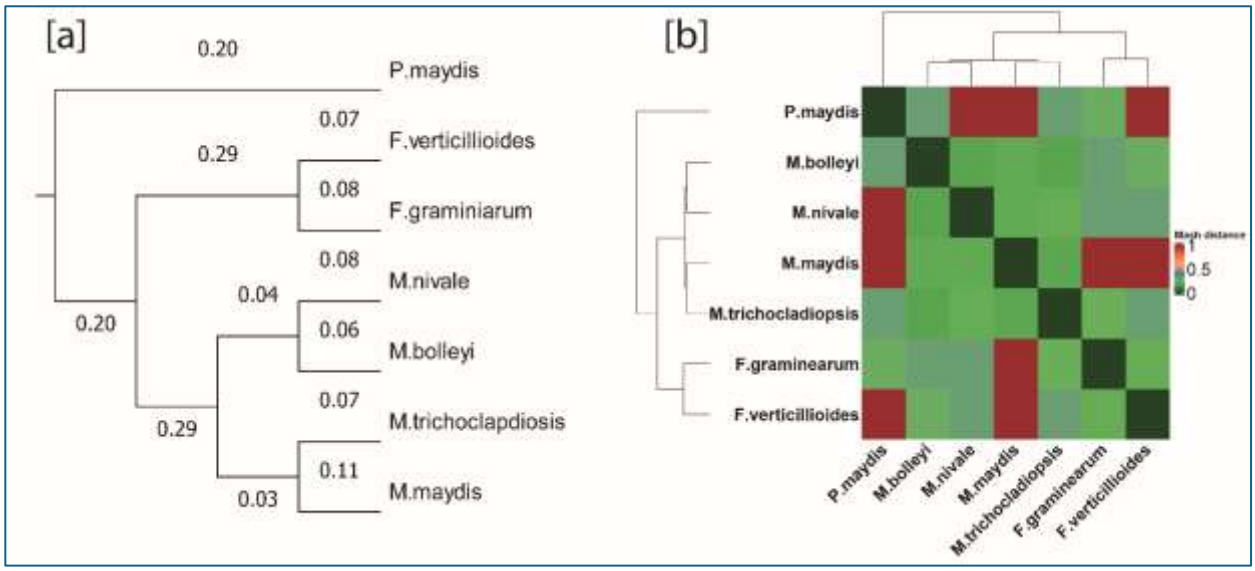


Figure 5: a) Phylogenetic relationships among M. maydis and related fungal species using whole proteome data, b) Heatmap indicating pairwise distance between species using the whole genome data.

Molecular markers to detect the presence of both species

We initially used ITS1 and ITS4 primers to characterize the *M. maydis* cultures. Sanger sequencing of the PCR amplicon and further BLAST analysis against our assembled genome identified unique regions on the contig 5 with 100% identity. Though these primers show binding sites in *A. flavus* genome, the amplicon length is longer (595 bp) than the shorter amplicon (561 bp) of *M. maydis* (Fig. 3). Interestingly, neither of the two primers have binding sites in the *P. maydis* genome, making them a suitable choice for identification of *M. maydis* in the tar spot complex while the earlier can be detected using our previously reported marker [15].

Conclusions

This study is the first comprehensive genetic characterization of *Monographella maydis,* a tar spot complex (TSC)-associated fungus. After successful *in vitro* culture, DNA isolation and high-quality genome sequencing, a complete and near-contiguous genome assembly was obtained. A robust list of predicted genes with their functional domains and potential virulence factors were derived, offering valuable insights into the molecular mechanisms that form the makeup of this species. Comparative analyses using phylogenomic approaches revealed that *M. maydis* shares evolutionary relationships with other members of the *Microdochium/Monographella* genus, while also showing that it has unique characteristics that could explain its specialization and role in the TSC.

Our analysis revealed the presence of a conserved H352 residue in the *M. maydis* ADA protein, which indicates its ability for A-to-I RNA editing required during sexual reproduction in filamentous fungi and their survival in comparison to *P. maydis,* which lacks the residue as well as the conserved domain. Finally, we have verified the usefulness of ITS1 and ITS4 primer pairs for PCR-based detection of *M. maydis* from the infected maize leaves.

Overall, this work establishes a genomic and analytical framework for *M. maydis*, opening new avenues for understanding the evolution, pathogenic potential, and adaptations of fungi involved in maize diseases. Future experimental approaches should aim to verify the role of ADA in sexual reproduction in both fungi.

Declarations

Authors declare no conflict of interest.

Materials and methods

Isolation of *M. maydis*

The morphological characteristics described by Müller & Samuels [10] were used as the basis of identification and isolation of *Monographella maydis* and its anamorph *Microdochium maydis* from the tar spot complex of maize leaves. Infected maize leaves exhibiting both tar spot and fisheye symptoms were collected from the CIMMYT Experimental Station in Poza Rica, Veracruz, Mexico, during the second agricultural cycle of 2022. The site was selected because of its favorable

climatic conditions for disease development and the persistence of the fungus in the soil as sclerotia [2, 18].

Leaf samples were then placed in humid chambers to promote stromatal hydration and fungal sporulation. Briefly, 1 × 1 sq. inch of dry tissue containing lesions with halos were cut and placed on petri dishes layered with moist filter paper. Unsealed petri dishes with the leaf discs were placed in a plastic box with wet paper towels at the bottom. The sealing of the petri dishes were avoided to maintain the humidity inside it without condensation. The plates were observed on daily basis to identify swollen hydrated stromata (Fig. 6).



Figure 6: Zone of sampling for the isolations.

After approximately one week, perithecia, formed on the leaf surface were isolated and transferred to petri dishes containing sterile media using a fine sterile needle. A small amount of ascospore was put into distilled water in a microfuge tube and mixed well by inversion. About 10 µl of this solution was added to another microfuge tube containing 900 µl of distilled water and mixed as before. This process was repeated several times to get a highly diluted preparation. Ten µl of this preparation was added to a water drop on a clean glass slide. The slide was briefly observed on a compound microscope to ensure that the fungal asci were clearly separated. It was allowed to air dry followed by a brief passage through a Bunsen burner for a few seconds to fix the asci on the slide with heat. A drop of methylene blue solution (1:4 v/v in water) was applied to the top of the fixed sample for staining. The slides were then rinsed with a soft stream of distilled water followed by air drying. A wax ring (paraffin wax) was placed around the sample to create a seal and the coverslip was applied to it. The slide was briefly warmed to set the coverslip and was stored in a sample box at room temperature for long term reference after labelling with the date and number of strains.

Optimization of the media and growth conditions

Spores were subsequently inoculated on four different media to assess the optimal growth media. Potato Dextrose Agar (PDA) (Himedia, USA) was the first choice since it is commonly used for isolation and growth of wide range of fungi [13, 55]. In addition to the commercial PDA media, we prepared and tested a natural Potato Dextrose Agar (PDAn). Briefly, 250 g of skinless potato was boiled in 750 ml of distilled water for 20 min in a pressure cooker. The water was filtered with cheese cloth and 20 g of Bacto-Agar, 10 g of Dextrose was added to the flowthrough. The volume was made upto 1L with distilled water and autoclaved for 15 min at 121°C, 15 PSI. Carnation Leaf Agar (CLA) (El Crisol, Mexico) was the next choice since it has been successfully used for culture of fungi [56]. Similarly, the V8 agar (V8) media has also been popularly used for culture of several fungal species [57, 58]. Our V8 media comprised Bacto-Agar 20 g/L, V8 original 100% vegetable

juice (V8 Juice brand from Walmart, Mexico) 200 ml/L, $CaCO_3$ 3g/L. The plates were incubated at 25°C with 12 h light / 12 h dark photoperiod and monitored every day. Contaminated plates discarded immediately.

Developing monosporic culture

A single sporodochium from the fungal plate was transferred with an insulin needle to a microfuge tube containing 1 ml of sterile distilled water. The tube was vortexed so that the sporodochium could release all the conidia. Once the solution appeared homogeneous, 20 µl of the solution was spread well in a petri dish carrying fungal media (any media available can be used in this step). An isolated conidium was located in the plate by observing under a compound microscope. The piece of media that contained the spore was taken out by using a sterile scalpel and placed on a petri dish containing V8 media which was found to be the best media to support the *M. maydis* growth in the previous experiment and grown as before.

DNA extraction of *M. maydis*

Several perithecia were aseptically transferred using an insulin needle to a sterile microfuge tube. These were suspended in sterile distilled water and macerated using sterile microtube pestles to release asci. Hundred µl of the asci solution was spread in a petri dish with V8 media and incubated for approximately 5-7 days at 25°C with 12 hours of light, and 12 hours of dark photoperiod. The white mycelia was scraped from the plate using a sterile pipette tip (200 µl) for DNA extraction (Fig. 2d).

Genomic DNA was extracted from freshly grown mycelium obtained from subcultures of isolates MNG128, MNG133, and MNG137 that showed clean and uniform growth without any contamination. The extraction process was challenging due to the complex fungal cell wall composition, primarily consisting of chitin, glucans, and glycoproteins [21, 59]. Therefore, the Quick-DNA™ Fungal/Bacterial Miniprep Kit (Zymo Research, USA) was used for the initial genomic DNA extraction. Though this DNA was good for PCR analysis, it was of low molecular weight (~5 kb), and the concentration was insufficient for long-read sequencing (Supplementary Fig. 2a).

An alternative protocol based on Phenol:Chloroform:Isoamyl alcohol (25:24:1) extraction was used to extract the fungal genomic DNA with slight modification [60]. This method proved more efficient and cost-effective, producing higher molecular weight DNA (>15 kb) suitable for third-generation sequencing (PacBio). Briefly, fresh fungal mycelia was pulverized in liquid N_2 using clean and sterile mortar and pestle. About 500 µl of the fungal mycelia powder (light pink to white colored) was transferred to a 2 ml microfuge tube with a sterile spatula and 600 µl prewarmed 2X CTAB extraction buffer (20mM EDTA, 1.4M NaCl, 100mM Tris-HCl, pH 8, 2% CTAB, 2% PVP) was added to it. The contents were mixed well by inversion and incubated at 65°C water bath for 30 - 60 min, while inverting every 10 min. Subsequently, the tube was cooled on the work bench and an equal volume (600 µl) of chilled phenol:chloroform:isoamyl alcohol (25:24:1) added to it in the fume hood. The contents were inverted several times by hand, followed by 5 min of mixing

in a rotor at room temperature (RT) and centrifuged at 14,000 rpm for 20 min at RT. The aqueous phase (750 µl approximately) was carefully transferred to a fresh 2 ml microfuge tube without disturbing the intermediate layer. It was mixed with another 800 µl of chloroform in a rotor for 3 min and centrifuged for 10 min at 14,000 rpm at RT. The final aqueous phase was transferred to a fresh 1.5 ml tube using a 200 µl pipette tip (precut to reduce the suction pressure).

To remove the RNA, three µl of RNase (10 mg/ml) (Qiagen, USA) was added to each tube and the contents were incubated at 37°C for 20-25 min. The DNA was precipitated by adding an equal volume (700 µl) of chilled 2-propanol (Sigma, USA) and mixed gently by inverting. High quality DNA threads were clearly visible, which were spooled and transferred to a fresh microfuge tube containing 1 ml of 70% (v/v) ethanol by using a sterile 200 µl tip. The DNA was reprecipitated by centrifuging at 13,000 rpm for 2 min. This step was repeated by discarding the supernatant, adding 500 µl of 70% (v/v) ethanol and centrifuging as above. The pellet was dried in the fume hood for 10 min and dissolved in 100 µl 1xTE, pH 8.0 (10 mM Tris-HCl and 1 mM EDTA). The DNA was left overnight at 4°C and the quality was checked by loading 4 µl of DNA in 1% agarose gel and running at 100 V (5V/cm) for an hour.

Estimation DNA concentration

For PacBio sequencing, the recommended input is approximately 3 µg of DNA per Gb of genome size. Considering the expected genome size for Ascomycota (~37 Mb), concentrations above 200 ng/µL and volumes above 100 µL were deemed suitable for sequencing [61, 62].

Given the possible interference of CTAB and phenol residues with spectrophotometric readings, DNA concentration was semi-quantitatively estimated by agarose gel electrophoresis. One microliter of each sample was loaded on a 1% agarose gel alongside a 1 Kb Plus DNA Ladder® (Thermo Fisher, USA, Catalog number 10787026). The relative band intensity when compared to the 1,500 bp reference band of the ladder allowed a semi-quantitative estimation (When 10 µl of Ladder (50 ng/µl) was loaded in a single lane, the 1,500 bp band represented approximately 70 ng) and so on. DNA from all three isolates showed higher concentrations than 210 ng/µl (Supplementary fig. 2b-d) and was used for PacBio sequencing.

Confirmation of *M. maydis* identity

Ribosomal Internal Transcribed Spacer (ITS) regions, which is located between the small subunit (SSU) and large subunit (LSU) rRNA genes is a hyper variable region and can be utilized for developing molecular markers for species identification and phylogenetic studies. The ITS primers are suggested as the most successful markers for identification for the broadest range of fungi and in determining inter- and intra-specific variation [63–66]. The ITS1, which hybridizes at the end of 18S rDNA, and ITS4 which hybridizes at the beginning of 28S rDNA have been successfully used to identify several fungal pathogens [67]. Therefore, these primer pairs were adopted for amplification of *M. maydis*.

Genomic DNA, previously extracted by the Quick-DNA™ Fungal/Bacterial Miniprep Kit from the mycelia of selected strains, was diluted to 20 ng/µl with nuclease free water and PCR amplified using primer pair ITS1 (5′-TCC GTA GGT GAA CCT GCG G-3′) and ITS4 (5′-TCC TCC GCT TAT TGA TAT GC-3′) [12, 64]. The 20 µl PCR reaction mixture comprised 1x reaction buffer, 250 µM each dNTP), 4.0 pmol of forward and reverse primers, 1 unit of GoTaq® DNA Polymerase (Promega, USA) and 50 ng of DNA template. The cycling parameters were 95°C for 1 min for initial denaturation followed by 32 cycles of denaturation at 95°C for 20 s, annealing at 55°C for 20 s and amplification at 72°C for 1 min. The final amplification was made for 5 min at 72°C.

For the Sanger sequencing, the PCR was repeated using a high-fidelity DNA polymerase. The 50 µl reaction mix comprised Phusion DNA polymerase (NEB, USA) 1 u, 1 x reaction buffer, 200 µM dNTP each, 20 picomoles of forward and reverse primers, 3% (v/v) Dimethyl sulfoxide (DMSO) and 2 µl of DNA template DNA. The reaction was carried out in a VeritiPro thermal cycler (Thermo Scientific, USA). The initial denaturation was performed at 98°C for 3 min followed by 35 cycles of denaturation at 98°C for 20s, annealing at 64°C for 20s and extension for 30 sec at 72°C. The final extension was performed for 5 min at 72°C. All PCR products were separated on 1% (w/v) agarose gels (SeaKem LE agarose, Lonza Bioscience, USA), stained with SYBR Safe gel stain (Thermofisher, USA) and documented in a gel doc (Bio-Rad, USA).

The target bands were excised by a scalpel and purified using the QIAquick Gel Extraction Kit (Qiagen, USA). The purified products, with concentrations between 70–80 ng/µl and $OD_{260/280}$ values ranging from 1.82 to 1.91, were sequenced externally at Macrogen Inc. (Seoul, Korea). The resulting sequences were analyzed using the BLASTn tool (NCBI), which confirmed their identity as *Monographella spp*.

Preservation of strains

To ensure long-term preservation and prevent loss of vitality or genetic drift, *M. maydis* isolates were cryopreserved [68]. Perithecia from each strain (MNG128, MNG133, MNG137) were suspended in sterile distilled water, homogenized, and mixed with equal volume of glycerol solution (1:1 v/v glycerol with either V8 medium or LB medium). Aliquots in 1.5 ml cryotubes were snap chilled in liquid N_2 and stored at –80°C freezer.

Whole genome sequencing

Sequencing strategy

High molecular weight genomic DNA, extracted from all three isolates (MNG128, MNG133, and MNG137) using the CTAB protocol, was sent to Novogene (USA) for whole-genome sequencing using the PacBio Sequel II DNA CLR library platform®. This method was chosen because long-read sequencing technologies overcome common challenges of *de novo* assembly such as coverage gaps and unresolved repetitive regions that often occur with short-read platforms [69]. The expected read length exceeded the so-called “golden threshold” of 7 kb, which is considered sufficient to resolve structural complexity and improve contiguity in *de novo* genome assemblies

[70]. Total 1,821,240 reads were generated ranging from 56 bp to 223,285 bp. The average genome coverage was about 250X.

Genome assembly and quality assessment

Since this was the first time *M. maydis* had been efficiently cultured *in vitro*, there were no previously available reference genomes. Reads with a mapping quality below 10 were filtered out prior to assembly. Genome assembly was performed using Canu, version 2.2, optimized for long-read data generated on the PacBio Sequel II platform [22]. A consensus genome assembly was performed combining the genome assemblies of all three replicates using programs such as Minimap2, SAMtools, BCFtools [71–73]. The consensus assembly was further polished using the software, Racon v1.5.0. Assembly quality and completeness were evaluated using BUSCO v5.5.0 fungal database (Ascomycota_odb10) [23] and QUAST v5.0 [25] (Supplementary table 1 and 2). The coding scripts used in the assembly and other analyses are available at: https://github.com/Sameerpokhrel1028/Monographella_maydis_Paper/tree/main.

Gene prediction and functional annotation

Structural and Functional Annotation

Gene prediction and structural annotation were performed on the assembled genome using the FunAnnotate pipeline (v1.8.15), optimized for fungal genome annotation [74]. Repetitive sequences were masked with FunAnnotate's masking tool before conducting the gene prediction (Supplementary fig. 9). This process used gene prediction tools such as AUGUSTUS, SNAP, GlimmerHMM, and GeneMark-ES, generating 10,228 predicted protein coding genes [75–78]. The rRNA prediction was conducted using Barrnap (v0.9) while the non-redundant ncRNAs were predicted using Infernal (v1.1.5) with the Rfam database.

The predicted protein coding sequences were then submitted to BLAST+ (v2.14.1) searches for homology and functional annotation. Protein sequences, extracted from the .gff3 file were queried against the UniProt protein database to identify homologous proteins and assign putative functions [78, 79]. A local BLAST database was generated from the UniProt dataset, and BLASTp was executed to compare the predicted protein sequences against it.

Predicted proteins were searched against the MEROPS peptidase database using DIAMOND BLASTP [80, 81]. For each query, only the top hit was retained. MEROPS annotation with a percent identity of more than 30%, bit score ≥ 100 and e-value $\leq 1e-20$ were defined as high confidence. Carbohydrate-active enzymes (CAZy) were identified using dbCAN (http://csbl.bmb.uga.edu/dbCAN/annotate.php) by integrating HMMER, DIAMOND, and dbCAN_sub predictions [82, 83].

Presence of signal peptides was predicted using SignalP 6.0 [84]. Analysis was conducted on all 10,228 predicted protein sequences from funannotate using default deep learning model and eukaryota as organism setting [84, 85].

Orthology analysis

Functional annotation and orthologous group identification were performed using EggNOG-mapper (v2.1.9), which assigns predicted proteins to orthologous groups and KEGG Orthology (KO) identifiers based on the eggNOG database [86, 87]. The predicted proteins from *M. maydis* were formatted in FASTA and analyzed, employing Diamond for fast sequence alignment against the eggNOG database [28]. This analysis generated annotations from KEGG Orthology, functional categories and metabolic pathway information. KEGG Mapper was used to visualize the annotated pathways [87].

Secondary metabolite analysis

The prediction of biosynthetic gene clusters (BGCs) and secondary metabolite pathways was performed using antiSMASH (v4.1.0) [88]. Although an attempt was made to execute *funannotate remote -m antismash*, the job was eventually completed by manually uploading the annotated GenBank file to the fungiSMASH server.

Phylogenomic analysis

To infer evolutionary relationships and identify conserved gene families, a comparative genomic analysis was conducted among three *Microdochium spp. (Microdochium bolleyi* (GCA_001566295), *Microdochium trichocladiopsis* (GCA_020744255), *Microdochium nivale* (GCA_026745475)), *Monographella maydis* (this study), common maize fungi such as *Fusarium gramenearum* (GCA900044135v1) and *Fusarium verticillioides* (ASM14955v1) and *Phyllachora maydis* (GCA_029339225) with which *M. maydis* co-colonizes in tar spot. The genomic data in GenBank (.gbff) format were downloaded from NCBI and analyzed using Get_Homologues (v14112024), employing the BBH, COG, and OrthoMCL algorithms to identify orthologous clusters [89]. A total of 2,034 core orthologous groups containing one protein per species were retained and further processed with Get_Phylomarkers (v2.8.1.4) [90].

A phylogenetic tree was constructed using the proteomes from all seven fungal genomes. The protein sequences were predicted for *M. maydis* as mentioned above and the reference protein sequence files for rest four pathogens were obtained from NCBI database. The software IQ-TREE (v3.0.1) was used to generate a species tree based on 1,000 bootstrap replicates [91]. The output phylogenetic tree represented the evolutionary relationship at the whole-proteome level and was visualized with MEGA v12.1 [92].

Mask sketch and mash dist were used to calculate the pairwise genetic distance using 32 CPU threads. The hierarchical clustering and heatmap visualization of the distance were performed using R v4.3.2 using the package ComplexHeatmap and circlize. A dendrogram was also included in the heatmap. The coloring was set to enhance the sensitivity to small genomic distances.

Keywords

Monographella maydis, Fisheye symptom, tar spot, RNA editing, genome assembly, sexual reproduction.

Ethics approval and consent to participate

Not applicable

Consent for publication

Not applicable

Availability of data and materials

Competing interests

The authors declare no conflict of interest. Views expressed in this work are solely those of the authors and not of the donor or affiliate organizations.

Authors' contributions

AKB and AEA developed the concept. AKB, SDA, LFG, SP, CMZ, IM and AEA performed experiments and data analysis. AKB, SDA and SP wrote the manuscript. POA and AEA reviewed and edited the manuscript. Everybody read and approved the manuscript.

Acknowledgements

Authors thank Mayolo Leyva Escalona for providing some of the samples used for the isolation of the *M. maydis* and M.C. Gabriela Juárez López for her support on isolation and culturing of the fungus. Authors also thank Dr. Luis Lasano for his critical input and support during the data analysis.

Funding

The authors would like to thank all donors who supported this work through their contributions to the CGIAR Fund (http://www.cgiar.org/whowe-are/cgiar-fund/fund-donors-2/), and in particular the ONE CGIAR Plant Health Initiative, now part of the Sustainable Intensification Initiative, for providing financial support for this research.

References

1. Jeschk M. Tar Spot of Corn in the U.S. and Canada. Crop Insights. 2026. https://www.pioneer.com/us/agronomy/Tar-Spot-of-Corn.html?utm_source=chatgpt.com. Accessed 9 Mar 2026.

2. INTAGRI. El Complejo de la Mancha de Asfalto en el Cultivo de Maíz. 2016. https://www.intagri.com/articulos/cereales/el-complejo-de-la-mancha-de-asfalto-en-el-cultivo-de-maiz.

3. Sol Hernández G. Diversidad genética de *Phyllachora maydis* y *Monographella maydis* y

668 respuesta del maíz a la inoculación artificial. Universidad Autonoma de Chipas; 2018.

669 4. Hock J, Dittrich U, Renfro BL, Kranz J. Sequential development of pathogens in the maize
670 tarspot disease complex. Mycopathologia. 1992;117:157–61.
671 https://doi.org/10.1007/BF00442777.

672 5. Groves CL, Kleczewski NM, Telenko DEP, Chilvers MI, Smith DL. *Phyllachora maydis*
673 ascospore release and germination from overwintered corn residue. Plant Heal Prog.
674 2020;21:26–30. https://doi.org/10.1094/PHP-10-19-0077-RS.

675 6. Valle-Torres J, Ross TJ, Plewa D, Avellaneda MC, Check J, Chilvers MI, et al. Tar spot: An
676 understudied disease threatening corn production in the Americas. Plant Dis. 2020;104:2541–50.
677 https://doi.org/10.1094/PDIS-02-20-0449-FE.

678 7. Crop Protection Network. Field Crop Disease Loss Calculator. 2025.
679 https://doi.org/10.31274/cpn-20191121-0.

680 8. Satyanarayana E. Importance of Maize and Utilisation. CornIndia. 2004.

681 9. Maublanc A. Especes nouvelles de champignons inferieurs. Bulletin de la Societe
682 Phytopathologique Franfaise. 1904;:72.

683 10. Müller, E.; Samuels GJ. Monographella maydis sp. nov. and its connection to the tar-spot
684 disease of *Zea mays*. Inst Microbiol. 1984;40:113–21.

685 11. Dittrich U, Hock J, Kranz J, Renfro B. Germination of *Phyllachora maydis* ascospores and
686 conidia of *Monographella maydis*. 1991. https://doi.org/10.5555/19942300411.

687 12. McCoy AG, Roth MG, Shay R, Noel ZA, Jayawardana MA, Longley RW, et al.
688 Identification of fungal communities within the tar spot complex of corn in Michigan via next-
689 generation sequencing. Phytobiomes J. 2019;3:235–43. https://doi.org/10.1094/PBIOMES-03-
690 19-0017-R.

691 13. Luis JM, Mehl HL, Plewa D, Kleczewski NM. Is *Microdochium maydis* associated with
692 necrotic lesions in the tar spot disease complex? A culture-based survey of maize in Mexico and
693 the midwestern United States. Phytopathology. 2023;113:1890–7.
694 https://doi.org/10.1094/PHYTO-04-23-0109-R.

695 14. Telenko DEP, Ross TJ, Shim S, Wang Q, Singh R. Draft genome sequence resource for
696 *Phyllachora maydis* - An obligate pathogen that causes tar spot of corn with recent economic
697 impacts in the United States. Mol Plant-Microbe Interact. 2020;33:884–7.
698 https://doi.org/10.1094/MPMI-03-20-0075-A.

699 15. Roggenkamp EM, Check JC, Biswal AK, Floyd CM, Miles LA, Nicolli CP, et al.
700 Development of a qPCR Assay for Species-Specific Detection of the Tar Spot Pathogen
701 *Phyllachora maydis*. PhytoFrontiers™. 2024;4:61–71. https://doi.org/10.1094/phytofr-04-23-
702 0050-fi.

703 16. Rogers A, Jaiswal N, Roggenkamp E, Kim HS, MacCready JS, Chilvers MI, et al. Genome-
704 informed trophic classification and functional characterization of virulence proteins from the
705 maize tar spot pathogen *Phyllachora maydis*. Phytopathology. 2024;114:1940–9.
706 https://doi.org/10.1094/PHYTO-01-24-0037-R.

17. Petrak F. Mykologische Notizen. VII. Ann Mycol. 1924;22.

18. Tronsmo AM, Collinge DB, Djurle A, Munk L, Yuen J, Tronsmo A. Plant pathology and plant diseases. 2020. p. 48–59.

19. Kumar M, Shukla PK. Use of PCR targeting of internal transcribed spacer regions and single-stranded conformation polymorphism analysis of sequence variation in different regions of rRNA genes in fungi for rapid diagnosis of mycotic keratitis. J Clin Microbiol. 2005;43:662–8. https://doi.org/10.1128/JCM.43.2.662-668.2005.

20. Toju H, Tanabe AS, Yamamoto S, Sato H. High-coverage ITS primers for the DNA-based identification of *Ascomycetes* and *Basidiomycetes* in environmental samples. PLoS One. 2012;7:e40863. https://doi.org/10.1371/journal.pone.0040863.

21. Lord A, Vyas J. Host defenses to fungal pathogens. In: Clinical Immunology. 2018.

22. Koren S, Walenz BP, Berlin K, Miller JR, Bergman NH, Phillippy AM. Canu: scalable and accurate long-read assembly via adaptive k -mer weighting and repeat separation. Genome Res. 2017;27:722–36. https://doi.org/10.1101/gr.215087.116.

23. Manni M, Berkeley M, Seppey M, Simao F, Zdobnov E. BUSCO update: novel and streamlined workflows along with broader and deeper phylogenetic coverage for scoring of eukaryotic, prokaryotic, and viral genomes. 2021. https://doi.org/arXiv:2106.11799 [q-bio] [Internet].

24. Simão FA, Waterhouse RM, Ioannidis P, Kriventseva E V., Zdobnov EM. BUSCO: Assessing genome assembly and annotation completeness with single-copy orthologs. Bioinformatics. 2015;31:3210–2. https://doi.org/10.1093/bioinformatics/btv351.

25. Gurevich A, Saveliev V, Vyahhi N, Tesler G. QUAST: quality assessment tool for genome assemblies. Bioinformatics. 2013. https://doi.org/10.1093/bioinformatics/btt086.

26. King R, Brown NA, Urban M, Hammond-Kosack KE. Inter-genome comparison of the Quorn fungus *Fusarium venenatum* and the closely related plant infecting pathogen *Fusarium graminearum*. BMC Genomics. 2018;19:1–19. https://doi.org/10.1186/s12864-018-4612-2.

27. Estrada R, Aragón L, Pérez WE, Romero Y, Martínez G, Garcia K, et al. Draft genome sequence data of *Fusarium verticillioides* strain REC01, a phytopathogen isolated from a Peruvian maize. Data Br. 2024;57:110951. https://doi.org/10.1016/j.dib.2024.110951.

28. Tarailo-Graovac M, Chen N. Using RepeatMasker to identify repetitive elements in genomic sequences. Curr Protoc Bioinforma. 2009; SUPPL. 25:1–14. https://doi.org/10.1002/0471250953.bi0410s25.

29. Chan PP, Lin BY, Mak AJ, Lowe TM. tRNAscan-SE 2.0: improved detection and functional classification of transfer RNA genes. Nucleic Acids Res. 2021;49:9077–96. https://doi.org/10.1093/nar/gkab688.

30. Yandell M, Ence D. A beginner's guide to eukaryotic genome annotation. Nat Rev Genet. 2012;13:329–42. https://doi.org/10.1038/nrg3174.

31. Seemann T. Microbial RNA annotation. GitHub. 2026. https://github.com/tseemann/barrnap.

745 Accessed 24 Apr 2026.

746 32. Zmasek CM, Godzik A. This Déjà Vu Feeling—Analysis of multidomain protein evolution
747 in eukaryotic genomes. PLoS Comput Biol. 2012;8:e1002701.
748 https://doi.org/10.1371/journal.pcbi.1002701.

749 33. Tordai H, Nagy A, Farkas K, Bányai L, Patthy L. Modules, multidomain proteins and
750 organismic complexity. FEBS J. 2005;272:5064–78.

751 34. Ahmed T, Juhász A, Bose U, Terefe NS, Colgrave ML. The role of fungal proteases in
752 bioactive peptide production and analytical approaches for tracking their activity. Trends Anal
753 Chem. 2025;192.

754 35. Liu F, Xiao J, Wang X-F, Wang Y-X, Yang H-H, Cai Y-B, et al. Role of carbohydrate-active
755 enzymes in brown planthopper virulence and adaptability. Front Plant Sci. 2025;16.
756 https://doi.org/10.3389/fpls.2025.1554498.

757 36. Liu H, Lu X, Li M, Lun Z, Yan X, Yin C, et al. Plant immunity suppression by an exo-β-1,3-
758 glucanase and an elongation factor 1α of the rice blast fungus. Nat Commun. 2023;14.

759 37. Munzert KS, Engelsdorf T. Plant cell wall structure and dynamics in plant–pathogen
760 interactions and pathogen defence. J Exp Bot. 2025;76:228–242.

761 38. Pan S, Tang L, Pan X, Qi L, Yang J. A member of the glycoside hydrolase family 76 is
762 involved in growth, conidiation, and virulence in rice blast fungus. Physiol Mol Plant Pathol.
763 2021;113 July 2020:101587. https://doi.org/10.1016/j.pmpp.2020.101587.

764 39. Laurian R, Dementhon K, Doumèche B, Soulard A, Noel T, Lemaire M, et al. Hexokinase
765 and glucokinases are essential for fitness and virulence in the pathogenic yeast *Candida albicans*.
766 Front Microbiol. 2019;10 FEB:1–18. https://doi.org/10.3389/fmicb.2019.00327.

767 40. Sahoo S, Rao KH. Role of carbon and nitrogen assimilation in *Candida albicans* survival and
768 virulence. Microbe (Netherlands). 2024;4 July:100127.
769 https://doi.org/10.1016/j.microb.2024.100127.

770 41. Guo B, Huo F, Huang F, Cui Y, Ling J, Song X. Naringenin inhibits the growth of *Diaporthe*
771 *citri* by targeting fungal glucokinase. J Agric Food Chem. 2025;73:28648–61.
772 https://doi.org/10.1021/acs.jafc.5c04212.

773 42. Wang S, Lin R, Tumukunde E, Zeng W, Bao Q, Wang S, et al. *Glutamine Synthetase*
774 contributes to the regulation of growth, conidiation, sclerotia development, and resistance to
775 oxidative Stress in the fungus *Aspergillus flavus*. Toxins (Basel). 2022;14.
776 https://doi.org/10.3390/toxins14120822.

777 43. Bian Z, Wang Z, Wang D, Xu J-R. Sexual stage–specific A-to-I mRNA editing is mediated
778 by tRNA-editing enzymes in fungi. Proc Natl Acad Sci. 2024;121:2017.
779 https://doi.org/10.1073/pnas.2319235121.

780 44. Liu H, Wang Q, He Y, Chen L, Hao C, Jiang C, et al. Genome-wide A-to-I RNA editing in
781 fungi independent of ADAR enzymes. Genome Res. 2016;26:499–509.
782 https://doi.org/10.1101/gr.199877.115.

783 45. Du Y, Jiang D, Liu H. RNA editing system: Balancing altruistic antiviral defense and fitness
784 trade-offs in fungi. mLife. 2025;4:599–603. https://doi.org/10.1002/mlf2.70057.

785 46. Bian Z, Ni Y, Xu JR, Liu H. A-to-I mRNA editing in fungi: occurrence, function, and
786 evolution. Cell Mol Life Sci. 2019;76:329–40. https://doi.org/10.1007/s00018-018-2936-3.

787 47. Feng C, Xin K, Du Y, Zou J, Xing X, Xiu Q, et al. Unveiling the A-to-I mRNA editing
788 machinery and its regulation and evolution in fungi. Nat Commun. 2024;15.
789 https://doi.org/10.1038/s41467-024-48336-8.

790 48. Xin K, Zhang Y, Fan L, Qi Z, Feng C, Wang Q, et al. Experimental evidence for the
791 functional importance and adaptive advantage of A-to-I RNA editing in fungi. Proc Natl Acad
792 Sci. 2023;120:2017. https://doi.org/10.1073/pnas.2219029120.

793 49. Medema MH, Kottmann R, Yilmaz P, Cummings M, Biggins JB, Blin K, et al. Minimum
794 Information about a Biosynthetic Gene cluster. Nat Chem Biol. 2015;11:625–31.
795 https://doi.org/10.1038/nchembio.1890.

796 50. Zhgun AA. Fungal BGCs for Production of Secondary Metabolites: Main Types, Central
797 Roles in Strain Improvement, and Regulation According to the Piano Principle. Int J Mol Sci.
798 2023;24. https://doi.org/10.3390/ijms241311184.

799 51. Tannous J, Labbé J, Keller NP. Identifying Fungal Secondary Metabolites and Their Role in
800 Plant Pathogenesis. Methods Mol Biol. 2023;2659:193–218. https://doi.org/10.1007/978-1-0716-
801 3159-1_15.

802 52. Pusztahelyi T, Holb IJ, Pócsi I. Secondary metabolites in fungus-plant interactions. Front
803 Plant Sci. 2015;6. https://doi.org/10.3389/fpls.2015.00573.

804 53. Motoyama T, Yun C-S, Osada H. Biosynthesis and biological function of secondary
805 metabolites of the rice blast fungus Pyricularia oryzae. J Ind Microbiol &biotechnology.
806 2021;23:9–10. https://doi.org/10.1093/jimb/kuab058.

807 54. Gao S, Li Y, Gao J, Suo Y, Fu K, Li Y, et al. Genome sequence and virulence variation-
808 related transcriptome profiles of Curvularia lunata, an important maize pathogenic fungus.
809 Springer Nat. 2014;15. https://doi.org/10.1186/1471-2164-15-627.

810 55. Uthayasooriyan M, Pathmanathan S, Ravimannan N, Sathyaruban S. Formulation of
811 alternative culture media for bacterial and fungal growth. Der Pharm Lett. 2016;8:444–9.

812 56. Fisher NL. Carnation leaves as a substrate and for preserving cultures of *Fusarium* species.
813 Phytopathology. 1982;72:151. https://doi.org/10.1094/phyto-77-151.

814 57. Hardina N, Kuswinanti T, Baharuddin. Modified vegetables extract as substitution of v8-
815 juice medium for cultivation of Phytophthora spp. IOP Conf Ser Earth Environ Sci. 2020;486.
816 https://doi.org/10.1088/1755-1315/486/1/012149.

817 58. Muhorakeye MC, Namikoye ES, Khamis FM, Wanjohi W, Akutse KS. Effective homemade
818 V8 juice formulation as alternative suitable medium for culturing Phytophthora infestans. Discov
819 Appl Sci. 2025;7. https://doi.org/10.1007/s42452-025-07495-z.

820 59. Dyakov Y, Ozeretskovskaya O. Vertical pathosystem: avirulence genes and their products.

In: Comprehensive and Molecular Phytopathology. 2007. p. 181–215.

60. Rajendrakumar P, Sujatha K, Rao KS, Natrajkumar P, Viraktamath BC, Balachandran SM, et al. A protocol for isolation of DNA suitable for rapid seed and grain purity assessments in rice. Rice Genet Newsl. 2006;23:92–5.

61. Mohanta TK, Bae H. The diversity of fungal genome. Biol Proced Online. 2015.

62. PacBio. Considerations for using the low and ultra-low DNA input workflows for whole genome sequencing. 2022.

63. Schoch CL, Seifert KA, Huhndorf S, Robert V, Spouge JL, Levesque CA, et al. Nuclear ribosomal internal transcribed spacer (ITS) region as a universal DNA barcode marker for Fungi. Proc Natl Acad Sci U S A. 2012;109:6241–6. https://doi.org/10.1073/pnas.1117018109.

64. Martin KJ, Rygiewicz PT, Rygioewicz P. Fungal-specific PCR primers developed for analysis of the ITS region of environmental DNA extracts. BMC Microbiol. 2005;5. https://doi.org/10.1186/1471-2180-5-28.

65. Tekpinar AD, Kalmer A. Utility of various molecular markers in fungal identification and phylogeny. Nov Hedwigia. 2019;109:187–224. https://doi.org/10.1127/nova_hedwigia/2019/0528.

66. Korabečná M, Liška V, Fajfrlík K. Primers ITS1, ITS2 and ITS4 detect the intraspecies variability in the internal transcribed spacers and 5.8S rRNA gene region in clinical isolates of fungi. Folia Microbiol (Praha). 2003;48:233–8. https://doi.org/10.1007/BF02930961.

67. Ferrer C, Colom F, Frasés S, Mulet E, Abad JL, Alió JL. Detection and identification of fungal pathogens by PCR and by ITS2 and 5.8S ribosomal DNA typing in ocular infections. J Clin Microbiol. 2001;39:2873–9. https://doi.org/10.1128/JCM.39.8.2873-2879.2001.

68. Crahay C, Declerck S, Colpaert J, Pigeon M, Munaut F. Viability of ectomycorrhizal fungi following cryopreservation. Fungal Biol. 2013.

69. Jang-il S, Jin-Wu N. The present and future of de novo whole-genome assembly. Brief Bioinform. 2018;Volume 19:23–40.

70. Koren S, Phillippy AM. One chromosome, one contig: complete microbial genomes from long-read sequencing and assembly. Curr Opin Microbiol. 2015;23:110–20. https://doi.org/https://doi.org/10.1016/j.mib.2014.11.014.

71. Danecek P, Bonfield JK, Liddle J, Marshall J, Ohan V, Pollard MO, et al. Twelve years of SAMtools and BCFtools. Gigascience. 2021;10:giab008. https://doi.org/10.1093/gigascience/giab008.

72. Li H, Handsaker B, Wysoker A, Fennell T, Ruan J, Homer N, et al. The Sequence Alignment/Map format and SAMtools. Bioinformatics. 2009;25:2078–9. https://doi.org/10.1093/bioinformatics/btp352.

73. Li H. Minimap2: pairwise alignment for nucleotide sequences. Bioinformatics. 2018;34:3094–100. https://doi.org/10.1093/bioinformatics/bty191.

74. Palmer JM, Stajich JE. Funannotate v1.8.1: Eukaryotic genome annotation. Zenodo. 2020.

https://doi.org/10.5281/zenodo.4054262.

75. Stanke M, Steinkamp R, Waack S, Morgenstern B. AUGUSTUS: a web server for gene finding in eukaryotes. Nucleic Acids Res. 2004;32:W309–12.

76. Bromberg Y, Rost B. SNAP: predict effect of non-synonymous polymorphisms on function. Nucleic Acids Res. 2007;35:3823–3835. https://doi.org/10.1093/nar/gkm238.

77. Majoros WH, Pertea M, Salzberg SL. TigrScan and GlimmerHMM: two open source ab initio eukaryotic gene-finders. Bioinformatics. 2004;20:2878–2879.

78. Ter-Hovhannisyan V, Lomsadze A, Chernoff Y, Borodovsky M. Gene prediction in novel fungal genomes using an ab initio algorithm with unsupervised training. Genome Res. 2008;18:1979–90. https://doi.org/10.1101/gr.081612.108.

79. The UniProt Consortium. UniProt: the Universal Protein Knowledgebase in 2025. Nucleic Acids Res. 2025;53:D609–D617.

80. Rawlings ND, Waller M, Barrett AJ, Bateman A. MEROPS: the database of proteolytic enzymes, their substrates and inhibitors. Nucleic Acids Res. 2014;42:D503–D509.

81. Buchfink B, Reuter K, Drost HG. Sensitive protein alignments at tree-of-life scale using DIAMOND. Nat Methods. 2021;18:366–8. https://doi.org/10.1038/s41592-021-01101-x.

82. Yin Y, Mao X, Yang J, Chen X, Mao F, Xu Y. DbCAN: A web resource for automated carbohydrate-active enzyme annotation. Nucleic Acids Res. 2012;40:445–51. https://doi.org/10.1093/nar/gks479.

83. Lombard V, Golaconda Ramulu H, Drula E, Coutinho PM, Henrissat B. The carbohydrate-active enzymes database (CAZy) in 2013. Nucleic Acids Res. 2014;42:D490–5. https://doi.org/10.1093/nar/gkt1178.

84. Teufel F, Armenteros JJA, Johansen AR, Gíslason MH, Pihl SI, Konstantinos D. Tsirigos, et al. SignalP 6.0 predicts all five types of signal peptides using protein language models. Nat Biotechnol. 2022;40:1023–5.

85. Mistry J, Chuguransky S, Williams L, Qureshi M, Salazar GA, Sonnhammer ELL, et al. Pfam: The protein families database in 2021. Nucleic Acids Res. 2021;49:D412–9. https://doi.org/10.1093/nar/gkaa913.

86. Cantalapiedra CP, Hernández-Plaza A, Letunic I, Bork P, Huerta-Cepas J. eggNOG-mapper v2: Functional Annotation, Orthology Assignments, and Domain Prediction at the Metagenomic Scale. Mol Biol Evol. 2021;38:5825–9. https://doi.org/10.1093/molbev/msab293.

87. Kanehisa M, Sato Y. KEGG Mapper for inferring cellular functions from protein sequences. Protein Sci. 2020;29:28–35. https://doi.org/10.1002/pro.3711.

88. Blin K, Shaw S, Villebro KSR, Ziemert N, Lee SY, Medema MH, et al. antiSMASH 5.0: updates to the secondary metabolite genome mining pipeline. Nucleic Acids Res. 2019.

89. Contreras-Moreira B, Vinuesa P. GET_HOMOLOGUES, a versatile software package for scalable and robust microbial pan-genome analysis. Appl Environ Microbiol. 2013;79:7696–701.

90. Vinuesa P, Ochoa-Sanchez L-E, Contreras-Moreira B. GET_PHYLOMARKERS, a software package to select optimal orthologous clusters for phylogenomics and inferring pan-genome phylogenies, used for a critical geno-taxonomic revision of the genus Stenotrophomonas. Front Microbiol. 2018;9. https://doi.org/doi: 10.3389/fmicb.2018.00771.

91. Wong T, Ly-Trong N, Ren H, Baños H, Roger A, Susko E, et al. IQ-TREE 3: Phylogenomic Inference Software using Complex Evolutionary Models. 2025. https://doi.org/10.32942/X2P62N.

92. Stecher G, Suleski M, Tao Q, Tamura K, Kumar S. MEGA 12.1: Cross-Platform Release for macOS and Linux Operating Systems. J Mol Evol. 2025;:14–8. https://doi.org/10.1007/s00239-025-10287-z.

Supplementary Files

This is a list of supplementary files associated with this preprint. Click to download.

- Supplementarytable4Functionalanalysisfinal.xlsx
- Supplementarymaterial.docx